

A Phase Adjustment Approach for Interference Reduction in OFDM-based Cognitive Radios

Ehsan Haj Mirza Alian and Patrick Mitran

University of Waterloo, Waterloo, Canada

Email: ealian@uwaterloo.ca, pmitran@ecemail.uwaterloo.ca

Abstract—The problem of cross-band interference in single-antenna and multi-antenna OFDM cognitive transmitters is considered. Cross-band interference, which is caused by large OFDM signal sidelobes, is a major drawback of OFDM, especially in cognitive radio applications where it is crucial to protect primary licensed users from the secondary user's interference. In this paper, we propose a novel low complexity technique, referred to as a *phase adjustment* technique, to tackle this problem in single-antenna and multi-antenna OFDM cognitive transmitters. In this technique, the phase of each OFDM symbol is adjusted in an attempt to minimize the interference caused by the secondary user to the primary. Unlike prior methods, this technique does not decrease data throughput and has no impact on the bit-error-rate and peak-to-average power ratio of the OFDM symbols. Furthermore, to calculate the adjustment phases, three heuristics, one of which is very low complexity and achieves near optimal performance in numerical simulations, are also proposed. In addition, performance of the proposed technique is evaluated analytically in some special cases in single and multi-antenna cognitive transmitters, and is verified by numerical simulations.

Index Terms—Cognitive radio, OFDM, interference cancellation, phase adjustment.

I. INTRODUCTION

ORTHOGONAL frequency division multiplexing (OFDM) is widely used in high data rate communication systems since it is robust against time dispersion in multipath fading channels and can be easily implemented. By dividing the total bandwidth into several parallel subchannels, OFDM also has the ability to adaptively allocate different bit rates and transmission powers to different subchannels and support the possibility of dynamic spectrum use. Hence, OFDM has been suggested as one of the best candidates for modulation in cognitive radio [2].

In OFDM-based cognitive radio systems, detected primary licensed users are protected by switching off the corresponding subcarriers of the secondary user which results in a non-contiguous OFDM system. However, OFDM has some major drawbacks such as large peak-to-average power ratio and high out-of-band radiation. The latter is mainly caused by sidelobes of the subcarriers that are produced because of symbol truncation in the time domain. Out-of-band radiation may thus cause interference to primary users in neighboring bands.

Currently, several sidelobe suppression techniques for OFDM-based cognitive systems have been addressed in the literature. Time domain windowing [3–5] is the simplest approach and lengthens the symbols with the help of using smooth shaping windows. As a downside, this reduces the useful data rate. Subcarrier weighting (SW) [6], on the other hand, weights all subcarriers in such a way as to minimize the sidelobe power. Since the data subcarriers are perturbed, this approach has the side effect of increasing the bit-error-rate (BER) of the system. In [7], the multiple choice sequences (MCS) approach is introduced to reduce the sidelobes of OFDM subcarriers. As in MCS, the index of the best sequence is required to be sent to the receiver, this technique effectively decreases the useful data rate. In the active interference cancellation (AIC) technique [8], a few subcarriers are reserved and weighted to suppress the sidelobes, whereas in the adaptive symbol transition (AST) method [9], this is achieved by adding an extension to time domain symbols which is optimized to reduce the sidelobes. However, both techniques mitigate the interference at the cost of a decrease in data throughput. Finally, the N-continuous OFDM approach [10] reserves a few subcarriers to create a smooth transition between consecutive OFDM symbols and thus, has the same shortcoming as the AIC technique.

OFDM can also be employed in multiple-antenna cognitive systems in order to increase system capacity and exploit diversity. However, only a few techniques in the literature have been proposed for sidelobe suppression in multiple-antenna OFDM transmitters and most are extensions of the AIC technique to multiple antennas. In [11], the authors apply the AIC method to all transmitter antenna symbols and compute the optimum value of cancellation tones jointly over multiple antennas. A more efficient extension of AIC for multi-antenna non-contiguous OFDM systems is presented in [12], where it is suggested to insert cancellation tones in the OFDM symbols of only one of the transmitter antennas in an attempt to cancel the interference produced by other antennas. Although the AIC method shows acceptable performance in creating deep spectrum notches, it has somewhat high computational complexity as it needs to solve a constrained convex optimization problem for each symbol. The problem is acute in multi-antenna OFDM cognitive transmitters as the number of cancellation subcarriers grows with the number of transmitter antennas. In [13], the authors apply the N-continuous OFDM technique to a multi-antenna transmitter OFDM cognitive system. However, this inevitably increases the bit-error-rate

These results were presented in part at IEEE WCNC'12, Paris, France, 1–4 April, 2012 [1]. This work was supported in part by the Natural Science and Engineering Research Council of Canada (NSERC) and by BlackBerry.

TABLE I
COMPARISON OF DIFFERENT PROPOSED TECHNIQUES FOR SIDELobe SUPPRESSION IN OFDM

| Research work | Advantage(s) | Disadvantage(s) |
|--|---------------------------------|---------------------------------------|
| Time domain windowing [3–5] | Low complexity, No BER increase | Throughput reduction |
| Subcarrier weighting (SW) [6] | No throughput reduction | High complexity, BER increase |
| Multiple choice sequences (MCS) [7] | No BER increase | High complexity, Throughput reduction |
| Active interference cancellation (AIC) [8, 11, 12] | No BER increase | High complexity, Throughput reduction |
| Adaptive symbol transition (AST) [9] | No BER increase | High complexity, Throughput reduction |
| N-continuous OFDM [10, 13] | No BER increase | Throughput reduction |

(BER) due to the precoder used at the transmitter to suppress the OFDM sidelobes, and explicit considerations are taken when the receiver has multiple antennas as well.

Although all of the abovementioned methods have shown relatively acceptable performance in interference mitigation, they all suffer from one or more of these shortcomings: high computational complexity, reduction in useful data throughput, and increase in BER. Advantages and disadvantages of the abovementioned techniques are summarized in Table I.

In this paper, we consider the problem of interference reduction in both single-antenna and multi-antenna OFDM cognitive transmitters. We propose a phase adjustment technique to reduce the interference power coming from the out-of-band radiation of the secondary OFDM system to the primary user, and the scheme is blind to the number of receiver antennas at the secondary user. We also evaluate the performance of the proposed technique in interference reduction analytically in some special cases for both single-antenna and multi-antenna secondary transmitters. The results related to the multi-antenna case were partially presented in our previous work [1], where a secondary transmitter with only two transmitter antennas is considered. In this paper, we generalize the proposed technique to the single-antenna case and multi-antenna with more than two secondary transmitter antennas.

For the multi-antenna cognitive transmitter case, the proposed technique rotates symbols transmitted from each antenna in the complex plane based on the symbols transmitted from other antennas at the same time. The optimal rotation phase of each antenna is computed such that, after passing through the channel, the total interference spectrum at the primary receiver due to all secondary antennas is minimized.

Since in the multi-antenna case the interference minimization is performed across the transmitter antennas, there should be at least two secondary transmitter antennas for this approach to work. Thus, for the single-antenna cognitive transmitter case, we propose a phase rotation technique that considers multiple consecutive OFDM symbols. In the proposed single-antenna technique, subcarriers of each OFDM symbol are rotated by an optimal phase, based on the previous OFDM symbols, such that the resulting interference due to the considered consecutive OFDM symbols is minimized, i.e., Welch's spectrum estimate of the transmitted OFDM symbol stream is minimized at the primary band. The approach of reducing the interference due to multiple consecutive symbols has been taken in some of prior works, e.g. [9, 10].

In some special cases, the optimal phase rotation can be calculated using a simple inner product. For the other cases, three

different novel and low complexity heuristics are presented for approximating the required rotation phases of the OFDM symbols. One of the heuristics, i.e., the block coordinate descent method, is found to achieve near optimal performance obtained by brute-force search, at very low complexity.

As noted above, in the single-antenna case, in contrast to the multi-antenna case, interference is minimized over different symbols which belong to consecutive transmission times. As explained in Section II-C, the performance analysis for the single-antenna case is then not a special case of the multi-antenna case with one transmitter antenna, and requires its own separate analysis.

Moreover, in the proposed techniques, all subcarriers of an OFDM symbol are rotated by the same phase. This phase can be regarded as part of a common phase (CP) which can be considered as a part of the channel effect known as common phase error (CPE), and is compensated for in any practical OFDM system. Therefore, the receiver can compensate for the phase rotation using one of the several methods that have been proposed for mitigating the CPE in the literature [14], [15]. As a result, the proposed phase adjustment method does not need explicit side information to be sent to the receiver for data recovery and data throughput is not decreased.

Finally, the phase adjustment method does not introduce any increase in bit-error-rate (BER) since it rotates all of the subcarriers by the same phase and thus, the location of the constellation points with respect to each other remain unchanged.

This paper is organized as follows. In Section II, the system model for the single-antenna cognitive system is introduced and the phase adjustment technique is proposed and analyzed. In Section III, we present the system model and the phase adjustment technique for the multiple-antenna cognitive system. Analysis of the technique is also presented in this section. Finally, numerical results and conclusion are given in Section IV and Section V, respectively.

II. SINGLE-ANTENNA OFDM COGNITIVE TRANSMITTER

A. System and Signal Model

A cognitive system with one transmit antenna employing non-contiguous OFDM signaling is considered. The cognitive receiver may have one or more antennas. The OFDM system is assumed to use a total of N subcarriers where some of them are switched off according to the detected primary user(s) activity. The transmitter block diagram is shown in Fig. 1. The input data bit stream is symbol-mapped resulting in a series

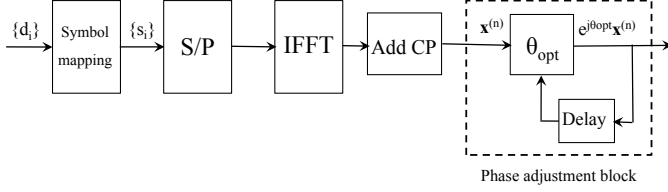


Fig. 1. Block diagram of the single-antenna phase adjusted OFDM cognitive transmitter.

of complex constellation points $\{s_i\}$ which are to modulate the active subcarriers.

The serial-to-parallel block converts the stream of $\{s_i\}$ into the complex-valued vector $\mathbf{X}^{(n)}$ where n is the symbol index. The cognitive engine deactivates the subcarriers that coincide with the primary user band according to the detected spectrum opportunity. $\mathbf{X}^{(n)}$ is then passed through the IFFT block resulting in

$$\hat{\mathbf{x}}^{(n)} = \frac{1}{N} W_{N,N}^\dagger \mathbf{X}^{(n)}, \quad (1)$$

where $W_{N,N} = [\omega^{kl}]$, $k, l = 0, \dots, N-1$, is the $N \times N$ discrete Fourier transform (DFT) matrix in which $\omega = e^{-j2\pi/N}$ and $(\cdot)^\dagger$ denotes the conjugate transpose.

To avoid intersymbol interference (ISI), the last G samples of $\hat{\mathbf{x}}^{(n)}$ are added at the beginning of the IFFT output, where G is assumed to be larger than the length of the channel impulse response. Therefore, the resulting time domain OFDM symbol can be expressed as

$$\mathbf{x}^{(n)} = \frac{1}{N} W_{N,N+G}^\dagger \mathbf{X}^{(n)}, \quad (2)$$

where $W_{N,N+G} = [A \ W_{N,N}]$ is a modified upsampled DFT matrix to include the cyclic prefix in which A is the submatrix of $W_{N,N}$ consisting of the last G columns of $W_{N,N}$.

In order to further decrease interference to the primary user, $\mathbf{x}^{(n)}$ is passed through the phase adjustment block that rotates each OFDM symbol by an appropriate phase.

To evaluate the spectrum in the primary band in-between the subcarrier frequencies, we use the upsampled FFT matrix defined as

$$W_{N,N}^{(L)} = [\omega^{kl/L}], \quad k = 0, \dots, N-1, \quad l = 0, \dots, NL-1, \quad (3)$$

where L is the upsampling factor. Hence, the upsampled spectrum of the n th OFDM symbol $\mathbf{X}^{(n)}$ is calculated as

$$\mathbf{X}_L^{(n)} = \frac{1}{N} W_{N,N+G}^{(L)} W_{N,N+G}^\dagger \mathbf{X}^{(n)}. \quad (4)$$

B. The Phase Adjustment Technique for Single-antenna OFDM Transmitter

The objective of the phase adjustment technique is to reduce the interference at the primary band by adjusting the phase of the transmitted OFDM symbols. In the phase adjustment technique for the single-antenna transmitter, all subcarriers of each OFDM symbol are rotated in the complex space by the same optimal phase to minimize the interference to the primary user.

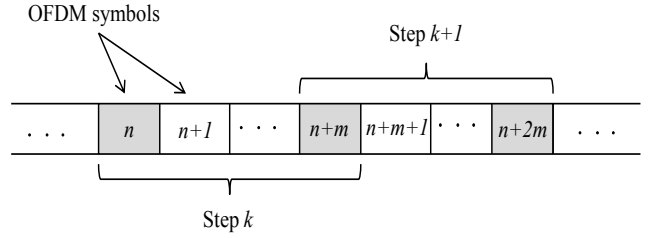


Fig. 2. Considering $m+1$ successive symbols in each step in the phase adjustment technique for single-antenna transmitter.

Considering $m+1$ successive OFDM symbols in each step, the optimal rotation phase of the last m symbols is computed in such a way that the entire interference of the $m+1$ symbols is minimized. The spectrum of the resulting symbols is computed using Welch's method [16], where a window length equal to $m+1$ OFDM symbols is considered for each spectrum estimation segment and the amount of overlap of the segments is one OFDM symbol, as shown in Fig. 2. Therefore, in each step, the first symbol's phase shift is assumed to be obtained by optimization from the previous step and thus, m optimal phases are to be calculated. Consequently, the $(m+1)$ th symbol in the current step will be considered as the first symbol in the next step.

Let $\mathbf{x}^{(n)}, \mathbf{x}^{(n+1)} \dots \mathbf{x}^{(n+m)}$ denote the $m+1$ consecutive OFDM symbols in the current step. The upsampled spectrum of the $m+1$ symbols is then calculated as

$$\mathbf{S}^{(n)} = W_{N,2(N+G)}^{(L)} \begin{bmatrix} \mathbf{x}^{(n)} \\ \vdots \\ \mathbf{x}^{(n+m)} \end{bmatrix} \quad (5)$$

$$= \sum_{i=0}^m D_i W_{N,N+G}^{(L)} \mathbf{x}^{(n+i)}, \quad (6)$$

where $D_i = \text{diag}\{e^{-2\pi jki(N+G)/NL}\}$, $k = 0, \dots, NL-1$.

Without loss of generality, we assume that the primary user occupies a bandwidth equivalent to B successive subcarriers $[X_{t+1}, X_{t+2}, \dots, X_{t+B}]$, where $B < N$. Thus, the interference vectors due to $\mathbf{x}^{(n)}, \dots, \mathbf{x}^{(n+m)}$ are expressed as

$$\mathbf{d}^{(n+i)} = \tilde{D}_i \tilde{W}_{N,N+G}^{(L)} \mathbf{x}^{(n+i)}, \quad i = 0, 1, \dots, m, \quad (7)$$

where $\tilde{W}_{N,N+G}^{(L)}$ is a submatrix of $W_{N,N+G}^{(L)}$ containing only the rows that correspond to the primary band, i.e., rows $(t+1)L$ through $(t+B)L$, and \tilde{D}_i is a submatrix of D_i defined as

$$\tilde{D}_i = \text{diag}\{e^{-2\pi jki(N+G)/NL}\}, \quad k = (t+1)L, \dots, (t+B)L.$$

In the proposed phase adjustment technique, the objective is to find the optimal rotation phase of the symbols $\mathbf{x}^{(n)}, \dots, \mathbf{x}^{(n+m)}$ to minimize the total interference of $[\mathbf{x}^{(n)\dagger} \mathbf{x}^{(n+1)\dagger} \dots \mathbf{x}^{(n+m)\dagger}]^\dagger$ to the primary user. Therefore, using a least square minimization criterion, the optimal rotation phase is calculated as

$$\theta_{\text{opt}} = \arg \min_{\theta} \|\mathbf{d}^{(n)} + e^{j\theta} \mathbf{d}^{(n+1)} + \dots + e^{j\theta m} \mathbf{d}^{(n+m)}\|^2, \quad (8)$$

which is a least squares (LS) optimization problem in which $\boldsymbol{\theta}_{\text{opt}} = [\theta_{1,\text{opt}} \cdots \theta_{m,\text{opt}}]^T$ is the set of optimal rotation phases of the considered symbols. The LS problem expressed in (8) can be reformulated as

$$\mathbf{a}_{\text{opt}} = \arg \min_{\mathbf{a}} \|\mathbf{d}^{(n)} + P\mathbf{a}\|^2, \quad (9)$$

$$\text{s.t. } |a_i|^2 = 1, \quad i = 1, \dots, m,$$

where $\mathbf{a} = [e^{j\theta_1}, \dots, e^{j\theta_m}]^T$ and $P = [\mathbf{d}^{(n+1)} \dots \mathbf{d}^{(n+m)}]$. Therefore, $\theta_i = \arg(a_i)$. The optimization problem defined in (9) is a least squares problem with multiple equality constraints.

For the special case of $m = 1$, the problem specializes as

$$\theta_{\text{opt}} = \arg \min_{\theta_1} \|\mathbf{d}^{(n)} + e^{j\theta_1} \mathbf{d}^{(n+1)}\|^2, \quad (10)$$

which is a single constraint LS minimization. Theorem 1 gives the solution to this problem.

Theorem 1: Given two arbitrary complex vectors $\mathbf{d}^{(n)}$ and $\mathbf{d}^{(n+1)}$ of the same length,

$$\theta = \pi - \arg\langle \mathbf{d}^{(n)}, \mathbf{d}^{(n+1)} \rangle \quad (11)$$

minimizes $\|\mathbf{d}^{(n)} + e^{j\theta} \mathbf{d}^{(n+1)}\|^2$, where $\langle \cdot, \cdot \rangle$ denotes the complex inner product. ■

Proof: See Appendix A. □

Therefore, according to Theorem 1, in the case of $m = 1$, the optimal rotation phase in the phase adjustment technique is simply found by calculating the inner product of the interference vectors, which implies that the complexity is very low.

In order to solve the problem for the general case of $m > 1$, we propose three algorithms, namely, a block coordinate descent (BCD) method, a greedy technique, and an opportunistic co-phase technique. The performance of these methods are evaluated in Section IV-A.

1) *Block coordinate descent (BCD) method:* The block coordinate descent or nonlinear Gauss-Seidel method is a suitable and efficient method for solving optimization problems where the cost function is continuously differentiable over the constraint set [17], which is true for the optimization problem defined in (9).

In the block coordinate descent method, the next iterate $\boldsymbol{\theta}^{k+1} = [\theta_1^{k+1}, \dots, \theta_m^{k+1}]^T$ is calculated according to the iteration

$$\theta_i^{k+1} = \arg \min_{\theta_i} \|\mathbf{d}^{(n)} + e^{j\theta_1^{k+1}} \mathbf{d}^{(n+1)} + \dots + e^{j\theta_{i-1}^{k+1}} \mathbf{d}^{(n+i-1)} + e^{j\theta_i} \mathbf{d}^{(n+i)} + e^{j\theta_{i+1}^k} \mathbf{d}^{(n+i+1)} + \dots + e^{j\theta_m^k} \mathbf{d}^{(n+m)}\|^2, \quad (12)$$

which can be simplified as

$$\theta_i^{k+1} = \arg \min_{\theta_i} \|\hat{\mathbf{d}}^{(n)} + e^{j\theta_i} \mathbf{d}^{(n+i)}\| \quad (13)$$

where $\hat{\mathbf{d}}^{(n)} = \mathbf{d}^{(n)} + e^{j\theta_1^{k+1}} \mathbf{d}^{(n+1)} + \dots + e^{j\theta_{i-1}^{k+1}} \mathbf{d}^{(n+i-1)} + e^{j\theta_{i+1}^k} \mathbf{d}^{(n+i+1)} + \dots + e^{j\theta_m^k} \mathbf{d}^{(n+m)}$. Equation (13) is then a single constraint LS minimization and has a *unique* solution which is calculated using Theorem 1 as

$$\theta_i^{k+1} = \pi - \arg\langle \hat{\mathbf{d}}^{(n)}, \mathbf{d}^{(n+i)} \rangle. \quad (14)$$

Algorithm 1: The Block Coordinate Descent Method for the Single-antenna Case

Result: Heuristic approximation $\boldsymbol{\theta}^*$ to the solution of (8). Compute $\mathbf{d}^{(n)}, \mathbf{d}^{(n+1)}, \dots, \mathbf{d}^{(n+m)}$ from (7);

Initialize $\boldsymbol{\theta}^0 = \mathbf{0}$

for $k = 1$ to Num-Iterations **do**

for $i = 1$ to m **do**

$$\left[\begin{array}{l} \hat{\mathbf{d}}^{(n,i)} = \mathbf{d}^{(n)} + e^{j\theta_1^k} \mathbf{d}^{(n+1)} + \dots + e^{j\theta_{i-1}^k} \mathbf{d}^{(n+i-1)} + \\ e^{j\theta_{i+1}^{k-1}} \mathbf{d}^{(n+i+1)} + \dots + e^{j\theta_m^{k-1}} \mathbf{d}^{(n+m)}, \\ \theta_i^k = \pi - \arg\langle \hat{\mathbf{d}}^{(n,i)}, \mathbf{d}^{(n+i)} \rangle. \end{array} \right.$$

$\boldsymbol{\theta}^* = \boldsymbol{\theta}^{\text{Num-Iterations}}$.

Furthermore, according to [17, proposition 2.7.1], every limit point of the sequence $\{\boldsymbol{\theta}^k\}$ generated by the BCD method is a stationary point of the objective function in (8). Finding a solution to (8) using the block coordinate descent method is summarized in Algorithm 1.

2) *Greedy technique:* This technique is a simple and fast technique for finding a suboptimal solution to (8). In the greedy technique, elements of the suboptimal solution $\boldsymbol{\theta}^*$ are calculated via solving

$$\begin{aligned} \theta_i^* &= \arg \min_{\theta_i} \|\mathbf{d}^{(n)} + e^{j\theta_1^*} \mathbf{d}^{(n+1)} + \dots + e^{j\theta_{i-1}^*} \mathbf{d}^{(n+i-1)} \\ &\quad + e^{j\theta_i} \mathbf{d}^{(n+i)} + \mathbf{d}^{(n+i+1)} + \dots + \mathbf{d}^{(n+m)}\|^2 \\ &= \arg \min_{\theta_i} \|\hat{\mathbf{d}}^{(n)} + e^{j\theta_i} \mathbf{d}^{(n+i)}\| \end{aligned} \quad (15)$$

where $\hat{\mathbf{d}}^{(n)} = \mathbf{d}^{(n)} + e^{j\theta_1^*} \mathbf{d}^{(n+1)} + \dots + e^{j\theta_{i-1}^*} \mathbf{d}^{(n+i-1)} + \mathbf{d}^{(n+i+1)} + \dots + \mathbf{d}^{(n+m)}$, and thus,

$$\theta_i^* = \pi - \arg\langle \hat{\mathbf{d}}^{(n)}, \mathbf{d}^{(n+i)} \rangle. \quad (16)$$

The greedy technique is in fact one iteration of the BCD method when initial phases are zero, and therefore, cannot outperform the BCD technique. However, it is faster and has less computational complexity.

3) *Opportunistic co-phase technique:* The technique is initially proposed in [18] to solve a problem of signal to interference and noise ratio (SINR) maximization in a multiple-input single-output (MISO) system. We exploit this technique here to find a suboptimal rotation phase vector of OFDM symbols to minimize the interference to the primary user.

Let $\{\boldsymbol{\theta}^i\}$, $i = 1, \dots, P$, be sets of candidate phase vectors to be employed in (8), where $\boldsymbol{\theta}^i = [\theta_1^i, \dots, \theta_m^i]^T$ and θ_j^i are random phases each chosen independently and uniformly over $[0, 2\pi)$. By defining $\mathbf{d}^i = \mathbf{d}^{(n)} + e^{j\theta_1^i} \mathbf{d}^{(n+1)} + \dots + e^{j\theta_m^i} \mathbf{d}^{(n+m)}$, then,

$$\hat{i} = \arg \min_{i=1, \dots, P} \|\mathbf{d}^i\|^2, \quad (17)$$

is the index of the phase vector that has the least interference to the primary user, i.e., $\boldsymbol{\theta}^{\hat{i}}$ is the algorithm's approximation of $\boldsymbol{\theta}_{\text{opt}}$. It is clear that by increasing the size of the phase set P , better approximations to $\boldsymbol{\theta}_{\text{opt}}$ are expected. Quantitative evaluation of the technique is presented in Section IV-A.

It is also worth noting that in the phase adjustment technique presented in this section, the phase rotation is the same for all

subcarriers within one OFDM symbol. This allows the receiver to consider the rotation as a part of the CPE. There are several methods in the literature for estimating the CPE (see e.g. [14], [15]). Hence, the transmitter doesn't need to send explicit side information along with data.

C. Performance Analysis

Based on the solutions provided in the previous section, only for the case of $m = 1$ there exists an analytical solution to (8). Therefore, in this section, the performance of the phase adjustment technique for $m = 1$ is analyzed. Note that because of the correlation structure of the interference vectors $\mathbf{d}^{(n)}$ and $\mathbf{d}^{(n+1)}$, as calculated in (22) and (23), the covariance matrices R_n and R_{n+1} cannot be diagonalized simultaneously. Hence, the performance analysis here is not a special case of that in Section III-C.

For the analysis, we first define the *improvement factor* as

$$\xi \triangleq \frac{\mathbb{E}\{\|\mathbf{d}^{(n)} + \mathbf{d}^{(n+1)}\|^2\}}{\mathbb{E}\{\min_{\theta} \|\mathbf{d}^{(n)} + e^{j\theta} \mathbf{d}^{(n+1)}\|^2\}}, \quad (18)$$

where $\mathbb{E}\{\cdot\}$ represents the expectation operator.

Entries of the interference vectors are the superposition of a relatively large number of sampled sidelobes of active subcarriers in the OFDM symbol with different weights. Thus, according to the central limit theorem, the interference vectors are approximated as *Gaussian* vectors. Assuming now that $\mathbf{d}^{(n)}$ and $\mathbf{d}^{(n+1)}$ are Gaussian, let R_n and R_{n+1} denote covariance matrices of $\mathbf{d}^{(n)}$ and $\mathbf{d}^{(n+1)}$, respectively, i.e.,

$$\begin{aligned} R_n &= \mathbb{E}\{\mathbf{d}^{(n)} \mathbf{d}^{(n)\dagger}\} \\ &= \widetilde{W}_{N,N+G}^{(L)} \mathbb{E}\{\mathbf{x}^{(n)} \mathbf{x}^{(n)\dagger}\} \widetilde{W}_{N,N+G}^{(L)\dagger}, \end{aligned} \quad (19)$$

and

$$\begin{aligned} R_{n+1} &= \mathbb{E}\{\mathbf{d}^{(n+1)} \mathbf{d}^{(n+1)\dagger}\} \\ &= \widetilde{D}_1 \widetilde{W}_{N,N+G}^{(L)} \mathbb{E}\{\mathbf{x}^{(n+1)} \mathbf{x}^{(n+1)\dagger}\} \widetilde{W}_{N,N+G}^{(L)\dagger} \widetilde{D}_1^\dagger \\ &= \widetilde{D}_1 R_n \widetilde{D}_1^\dagger, \end{aligned} \quad (20)$$

where (19) and (20) follow from (7). Using matrix diagonalization, we have

$$R_n = U \Sigma U^\dagger, \quad (22)$$

$$R_{n+1} = \widetilde{D}_1 U \Sigma U^\dagger \widetilde{D}_1^\dagger, \quad (23)$$

where $\Sigma = \text{diag}(\lambda_i)$, $i = 1, \dots, K$, is the eigenvalues matrix, K is the length of interference vectors, and $U = [\mathbf{u}_1 \ \mathbf{u}_2 \ \dots \ \mathbf{u}_K]$ is the eigenvectors matrix of R_n which is unitary since R_n is Hermitian. Thus, $\mathbf{d}^{(n)}$ and $\mathbf{d}^{(n+1)}$ can be expressed as

$$\mathbf{d}^{(n)} = U \mathbf{a}, \quad (24)$$

$$\mathbf{d}^{(n+1)} = \widetilde{D}_1 U \mathbf{b}, \quad (25)$$

where a_i and b_i are i.i.d Gaussian random variables with $a_i, b_i \sim \mathcal{CN}(0, \lambda_i)$, $i = 1, \dots, K$. The following theorem gives an upper bound on the improvement factor ξ .

Theorem 2: The improvement factor ξ , defined in (18), is upperbounded as

$$\xi \leq \frac{\sum_{i=1}^K \lambda_i}{\sum_{i=1}^K \lambda_i - [\text{Tr}(R_n R_{n+1})]^\frac{1}{2}}, \quad (26)$$

where $\text{Tr}(\cdot)$ denotes the matrix trace. \blacksquare

Proof: See Appendix B. \square

As Theorem 2 states, the upper bound depends only on the covariance matrices of the interference vectors. Each interference vector can be written as

$$\mathbf{d}^{(n)} = \sum_{i=1}^{N_a} X_i^{(n)} \mathbf{s}_i, \quad (27)$$

in which N_a is the number of active subcarriers, $X_i^{(n)}$ is the complex weight of the i^{th} subcarrier which we assume to be a zero-mean random variable with variance $\sigma_X^2 = 1$, and \mathbf{s}_i is the sampled tail of the i^{th} subcarrier in the primary band. Therefore,

$$R_n = \sum_{i=1}^{N_a} \sum_{j=1}^{N_a} (\mathbb{E}\{X_i^{(n)} X_j^{*(n)}\}) \mathbf{s}_i \mathbf{s}_j^\dagger = \sum_{i=1}^{N_a} \mathbf{s}_i \mathbf{s}_i^\dagger, \quad (28)$$

where (28) follows from the fact that $X_i^{(n)}$'s are i.i.d. and zero-mean with $\sigma_X^2 = 1$. Therefore, the covariance matrix does not depend on the data symbols and can be calculated separately. It depends only on the location of active subcarriers or, in other words, on the configuration of the primary user activity. In Section IV, we numerically calculate the improvement factor as well as the upper bound for different configurations of primary activity and show that the derived upper bound is relatively tight.

III. MULTI-ANTENNA OFDM COGNITIVE TRANSMITTER

A. System and Signal Model

In this section, we consider a multi-antenna OFDM cognitive transmitter. More specifically, it is assumed that the cognitive transmitter employs $M+1$ antennas to send information to the secondary receiver, and the secondary receiver has one or more antennas. A primary user is also assumed to receive the secondary signals and therefore is to be protected from the secondary user's interference, as shown in Fig. 3.

For the signals transmitted from each antenna, we assume the same model as in Section II-A, except the index used to denote the antenna from which the signal is being transmitted, i.e.,

$$\mathbf{x}_i^{(n)} = \frac{1}{N} W_{N,N+G}^\dagger \mathbf{X}_i^{(n)}, \quad i = 0, 1, \dots, M, \quad (29)$$

and

$$\mathbf{X}_{L,i}^{(n)} = \frac{1}{N} W_{N,N+G}^{(L)} W_{N,N+G}^\dagger \mathbf{X}_i^{(n)}, \quad i = 0, 1, \dots, M, \quad (30)$$

where $\mathbf{X}_i^{(n)}$ and $\mathbf{x}_i^{(n)}$ denote the n^{th} OFDM symbol transmitted from the i^{th} antenna in the frequency and time domain respectively, and $\mathbf{X}_{L,i}^{(n)}$ is the corresponding upsampled spectrum by a factor of L . Furthermore, we assume that $\mathbf{X}_0^{(n)}, \dots, \mathbf{X}_M^{(n)}$ are uncorrelated transmissions.

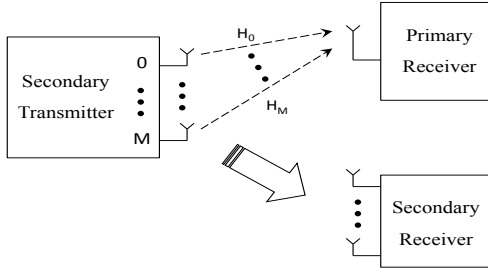


Fig. 3. System model of a multiple-antenna cognitive system.

Similar to Section II-A, we assume that the primary user occupies a bandwidth equivalent to B subcarriers among the total N subcarriers of the OFDM cognitive system.

Furthermore, let H_i , $i = 0, \dots, M$, be diagonal matrices that denote the channel matrix containing the frequency response in the primary band of the channel between the i th secondary transmitter antenna and the primary receiver antenna and these are assumed to be known to the cognitive system. Thus, H_i , $i = 0, \dots, M$, are diagonal $[(B-1)L+1] \times [(B-1)L+1]$ matrices.

B. The Phase Adjustment Technique for Multi-antenna OFDM Transmitter

For the multi-antenna cognitive transmitter case, to reduce interference to the primary user, the phase of each OFDM symbol is adjusted based on the symbols of the other transmitter antennas.

According to the system model described in Section III-A, the interference vector of the n th OFDM symbol due to the i th antenna at the secondary transmitter is

$$\mathbf{d}_{x_i}^{(n)} = \frac{1}{N} \widetilde{W}_{N,N+G}^{(L)} W_{N,N+G}^\dagger \mathbf{X}_i^{(n)}, \quad i = 0, 1, \dots, M. \quad (31)$$

In the multi-antenna case, since signals transmitted from different antennas undergo different channels, it is important to consider the effect of the channels and minimize the total received interference power at the location of the primary receiver. Otherwise, minimizing the interference before the effect of the channel does not necessarily help to reduce the interference to the primary user. This is in comparison to the single-antenna case, where a reduction in the spectrum before the channel always results in a reduction in the spectrum after the channel.

Here, the total interference at the primary receiver is the sum of the received interference spectrum due to each secondary transmitter antenna. Therefore, the interference vector at the primary receiver is

$$\mathbf{d}^{(n)} = \sum_{i=0}^M \mathbf{d}_{y_i}^{(n)}, \quad (32)$$

where

$$\mathbf{d}_{y_i}^{(n)} = H_i \mathbf{d}_{x_i}^{(n)}, \quad i = 0, \dots, M, \quad (33)$$

is the interference vector at the primary receiver due to the i th secondary transmitter antenna.

Algorithm 2: The Block Coordinate Descent Method for the Multiple-antenna Case

Result: A heuristic approximation θ^* to the solution of (34).

Compute $\mathbf{d}_{y_0}^{(n)}, \mathbf{d}_{y_1}^{(n)}, \dots, \mathbf{d}_{y_M}^{(n)}$ from (33) and (31);

Initialize $\theta^0 = \mathbf{0}$

for $k = 1$ to Num-Iterations **do**

for $i = 1$ to M **do**

$$\begin{aligned} \tilde{\mathbf{d}}^{(n,i)} &= \mathbf{d}_{y_0}^{(n)} + e^{j\theta_1^k} \mathbf{d}_{y_1}^{(n)} + \dots + e^{j\theta_{i-1}^k} \mathbf{d}_{y_{i-1}}^{(n)} + \\ & e^{j\theta_{i+1}^{k-1}} \mathbf{d}_{y_{i+1}}^{(n)} + \dots + e^{j\theta_M^{k-1}} \mathbf{d}_{y_M}^{(n)}, \\ \theta_i^k &= \pi - \arg\langle \tilde{\mathbf{d}}^{(n,i)}, \mathbf{d}_{y_i}^{(n)} \rangle. \end{aligned}$$

$\theta^* = \theta^{\text{Num-Iterations}}$.

In the proposed phase rotation technique for the multiple-antenna cognitive case, in order to reduce the interference to the primary user, OFDM symbols transmitted from each antenna of the secondary transmitter are rotated based on the symbols of other antennas such that the total interference power at the primary receiver is minimized. Thus, the optimal rotation phase that minimizes the interference at the primary receiver is computed as

$$\theta_{\text{opt}} = \arg \min_{\theta} \|\mathbf{d}_{y_0}^{(n)} + e^{j\theta_1} \mathbf{d}_{y_1}^{(n)} + \dots + e^{j\theta_M} \mathbf{d}_{y_M}^{(n)}\|^2, \quad (34)$$

where $\theta_{\text{opt}} = [\theta_1, \dots, \theta_M]^T$ is the optimal rotation phase of the transmitter antennas. Similar to Section II-B, the LS minimization expressed in (34) can be reformulated as an LS minimization with multiple equality constraints. Therefore, to the best of our knowledge, no analytical solution for this optimization problem is known in general that gives a closed form expression.

However, for the special case of $M = 1$, i.e. two transmitter antennas, (34) specializes as

$$\theta_{\text{opt}} = \arg \min_{\theta_1} \|\mathbf{d}_{y_0}^{(n)} + e^{j\theta_1} \mathbf{d}_{y_1}^{(n)}\|^2, \quad (35)$$

and, according to Theorem 1, θ_{opt} is calculated as

$$\theta_{\text{opt}} = \pi - \arg\langle \mathbf{d}_{y_0}^{(n)}, \mathbf{d}_{y_1}^{(n)} \rangle. \quad (36)$$

Therefore, similar to Section II-B, the proposed technique has low complexity in this case.

Since the minimization problem defined in (34) has the same structure as (8), the three techniques proposed in Section II-B can be used here to solve (34) in the general case of $M > 1$. Here we summarize these techniques in Algorithm 2, 3, and 4.

Moreover, similar to Section II-B, the proposed technique does not need explicit side information to be sent along with the data, since it can be absorbed as a part of channel effect in the form of a common phase error.

In the following section, the improvement in interference reduction achieved by the phase adjustment technique is analytically investigated for the case of $M = 1$, i.e. two antennas, since only for this case an analytical solution exists. Evaluation of other cases using the proposed techniques are presented in Section IV-B.

Algorithm 3: The Greedy Technique for the Multiple-antenna Case

Result: A heuristic approximation θ^* to the solution of (34).

Compute $\mathbf{d}_{y_0}^{(n)}, \mathbf{d}_{y_1}^{(n)}, \dots, \mathbf{d}_{y_M}^{(n)}$ from (33) and (31);

for $i = 1$ to M **do**

$$\begin{cases} \tilde{\mathbf{d}}^{(n)} = \\ \mathbf{d}_{y_0}^{(n)} + e^{j\theta_1^*} \mathbf{d}_{y_1}^{(n)} + \dots + e^{j\theta_{i-1}^*} \mathbf{d}_{y_{i-1}}^{(n)} + \mathbf{d}_{y_{i+1}}^{(n)} + \dots + \mathbf{d}_{y_M}^{(n)}, \\ \theta_i^* = \pi - \arg(\tilde{\mathbf{d}}^{(n)}, \mathbf{d}_{y_i}^{(n)}). \end{cases}$$

Algorithm 4: The Opportunistic Co-phase Technique for the Multiple-antenna Case

Result: A heuristic approximation θ^* to the solution of (34).

Compute $\mathbf{d}_{y_0}^{(n)}, \mathbf{d}_{y_1}^{(n)}, \dots, \mathbf{d}_{y_M}^{(n)}$ from (33) and (31);

for $k = 1$ to P **do**

for $l = 1$ to M **do**

└ Generate random $\theta_l^k \sim U[0, 2\pi)$

└ $\mathbf{d}^k = \mathbf{d}_{y_0}^{(n)} + e^{j\theta_1^k} \mathbf{d}_{y_1}^{(n)} + \dots + e^{j\theta_M^k} \mathbf{d}_{y_M}^{(n)}$

$\hat{k} = \arg \min_{k=1, \dots, P} \|\mathbf{d}^k\|^2,$

$\theta^* = \theta^{\hat{k}}$

C. Performance Analysis

The performance of the proposed phase rotation technique is analyzed in this section. Note that the analysis here is different than of the single-antenna case as now the interference vectors have the same statistics, i.e. the corresponding covariance matrices can be simultaneously diagonalized. This allows for a stronger analysis of the performance of the proposed method for the multi-antenna case. For analytical tractability, it is assumed that the secondary transmitter employs two antennas and the channels between the secondary transmitter antennas and the primary receiver are flat fading channels, i.e.,

$$H_i = h_i I, \quad i = 0, 1, \quad (37)$$

where h_i is the Rayleigh flat fading gain which we model by a zero-mean unit-variance complex Gaussian random variable, and I is the identity matrix. This assumption would be valid when the delay spread of the channel is small, specifically when there exists a line of sight between the transmitter and the receiver. Frequency selective fading channels are investigated numerically in the next section, where it is found that the performance of the proposed scheme is in line with the analytical predictions for flat fading channels.

In order to analyze the performance of the proposed technique in interference reduction, we use the improvement factor defined in (18) for the multiple-antenna scenario, i.e.,

$$\xi \triangleq \frac{\mathbb{E}\{\|\mathbf{d}_{y_0}^{(n)} + \mathbf{d}_{y_1}^{(n)}\|^2\}}{\mathbb{E}\{\min_{\theta} \|\mathbf{d}_{y_0}^{(n)} + e^{j\theta} \mathbf{d}_{y_1}^{(n)}\|^2\}}. \quad (38)$$

In the multi-antenna case, similar to the single-antenna case, OFDM interference vectors at the secondary transmitter side

can be approximated as *correlated Gaussian* vectors according to the central limit theorem. However, in this case, covariance matrices of the interference vectors $\mathbf{d}_{x_0}^{(n)}$ and $\mathbf{d}_{x_1}^{(n)}$ are the same and expressed as

$$R_{x_i} = \widetilde{W}_{N,N+G}^{(L)} \mathbb{E}\{\mathbf{x}_i^{(n)} \mathbf{x}_i^{(n)\dagger}\} \widetilde{W}_{N,N+G}^{(L)\dagger}, \quad i = 0, 1. \quad (39)$$

Therefore, the received interference vectors at the primary receiver are also approximated as correlated Gaussian vectors with covariance matrices

$$R_{y_i} = \mathbb{E}\{\mathbf{d}_{y_i}^{(n)} \mathbf{d}_{y_i}^{(n)\dagger}\} = |h_i|^2 R_{x_i}, \quad i = 0, 1. \quad (40)$$

The following theorem gives an approximation of the improvement factor of OFDM interference vectors $\mathbf{d}_{y_0}^{(n)}$ and $\mathbf{d}_{y_1}^{(n)}$. We use this approximation to obtain the improvement of the proposed technique in interference reduction to the primary user in Theorem 4.

Theorem 3: Assume that R_{y_0} (and R_{y_1}) have $l < K$ dominant eigenvalues, i.e.,

$$\lambda_1 \geq \dots \geq \lambda_l \gg \lambda_{l+1} \geq \dots \lambda_K, \quad (41)$$

where λ_i , $i = 1, \dots, K$, are eigenvalues of R_{y_0} (and R_{y_1}), and $K = (B-1)L + 1$ is the length of the interference vectors $\mathbf{d}_{y_0}^{(n)}$ and $\mathbf{d}_{y_1}^{(n)}$. Then,

$$\frac{\mathbb{E}\{\|\mathbf{d}_{y_0}^{(n)} + \mathbf{d}_{y_1}^{(n)}\|^2\}}{\mathbb{E}\{\min_{\theta} \|\mathbf{d}_{y_0}^{(n)} + e^{j\theta} \mathbf{d}_{y_1}^{(n)}\|^2\}} \approx \frac{\mathbb{E}\{\|\tilde{\mathbf{d}}_{y_0}^{(n)} + \tilde{\mathbf{d}}_{y_1}^{(n)}\|^2\}}{\mathbb{E}\{\min_{\theta} \|\tilde{\mathbf{d}}_{y_0}^{(n)} + e^{j\theta} \tilde{\mathbf{d}}_{y_1}^{(n)}\|^2\}}, \quad (42)$$

where

$$\tilde{\mathbf{d}}_{y_j}^{(n)} = [\tilde{d}_{j1}, \tilde{d}_{j2}, \dots, \tilde{d}_{jl}]^T, \quad j = 0, 1, \quad (43)$$

and $\tilde{d}_{0i} \sim \mathcal{CN}(0, \lambda_i)$, $\tilde{d}_{1i} \sim \mathcal{CN}(0, \frac{|h_1|^2}{|h_0|^2} \lambda_i)$, $i = 1, \dots, l$, are independent complex Gaussian random variables. The approximation in (42) becomes equality when $\frac{\lambda_{l+1}}{\lambda_l} \rightarrow 0$. ■

Proof: See Appendix C. □

According to Theorem 3, the improvement factor of the OFDM interference vectors $\mathbf{d}_{y_0}^{(n)}$ and $\mathbf{d}_{y_1}^{(n)}$ can be approximated as the improvement factor of complex Gaussian vectors of length l with *independent* entries, where l here is the number of dominant eigenvalues of the covariance matrices R_{y_0} and R_{y_1} .

Now, in order to investigate the number of dominant eigenvalues of R_{y_i} , $i = 0, 1$, we define the *eigenvalue ratio (ER)* as

$$\text{ER}(l) = \frac{\sum_{i=1}^l \lambda_i}{\sum_{i=1}^K \lambda_i}. \quad (44)$$

According to (28), the covariance matrices do not depend on the data symbols and the ER can be calculated separately. Indeed, the covariance matrices statistically depend only on the configuration of detected primary user spectrum. Hence, we run numerical simulations for different spectral opportunity configurations to investigate the behavior of the ER as a function of l . The result is shown in Fig. 4 where B is the number of deactivated subcarriers due to the detected primary user bandwidth. It is observed from Fig. 4 that for

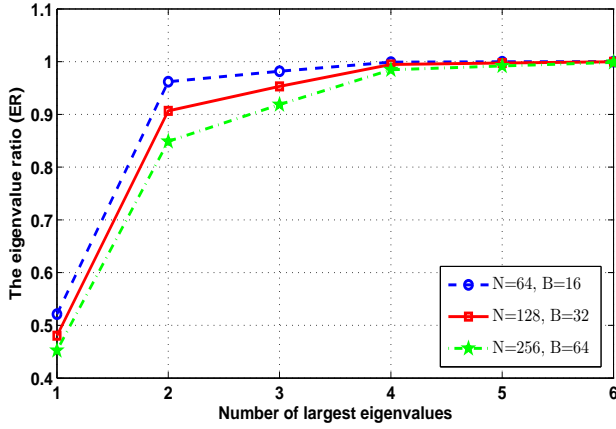


Fig. 4. The eigenvalue ratio (ER).

all configurations,

$$\lambda_1 \approx \lambda_2 \gg \lambda_3 \geq \dots \geq \lambda_K, \quad (45)$$

since $ER(2) \geq 0.85$ (and in some configurations $ER(2) \geq 0.95$). In other words, it can be concluded that $R_{\mathbf{y}_0}$ and $R_{\mathbf{y}_1}$ have $l = 2$ almost equal dominant eigenvalues. This is intuitively true, because, due to the diminishing tail of active subcarriers, most of the interference is produced by sidelobes of the nearest subcarriers to the primary band, namely one subcarrier on each side of the primary band.

Therefore, according to Theorem 3, the improvement factor of the interference vectors $\mathbf{d}_{\mathbf{y}_0}^{(n)}$ and $\mathbf{d}_{\mathbf{y}_1}^{(n)}$ is approximated as the improvement factor of two i.i.d. complex Gaussian vectors of length 2 defined as

$$\tilde{d}_{0i} \sim \mathcal{CN}(0, \lambda_1), \quad i = 1, 2, \quad (46)$$

$$\tilde{d}_{1i} \sim \mathcal{CN}(0, \frac{|h_1|^2}{|h_0|^2} \lambda_1), \quad i = 1, 2. \quad (47)$$

In Theorem 4, we calculate the improvement factor of i.i.d. complex Gaussian vectors.

Theorem 4: Let $\tilde{\mathbf{d}}_{\mathbf{y}_0}^{(n)}$ and $\tilde{\mathbf{d}}_{\mathbf{y}_1}^{(n)}$ be two zero-mean i.i.d. complex Gaussian random vectors of length l with entries $\tilde{d}_{0i} \sim \mathcal{CN}(0, \lambda_1)$ and $\tilde{d}_{1i} \sim \mathcal{CN}(0, \frac{|h_1|^2}{|h_0|^2} \lambda_1)$, $i = 1, \dots, l$. Then,

$$\frac{\mathbb{E}\{\|\tilde{\mathbf{d}}_{\mathbf{y}_0}^{(n)} + \tilde{\mathbf{d}}_{\mathbf{y}_1}^{(n)}\|^2\}}{\mathbb{E}\{\min_{\theta} \|\tilde{\mathbf{d}}_{\mathbf{y}_0}^{(n)} + e^{j\theta} \tilde{\mathbf{d}}_{\mathbf{y}_1}^{(n)}\|^2\}} = \frac{l[1 + \frac{|h_1|^2}{|h_0|^2}]}{l[1 + \frac{|h_1|^2}{|h_0|^2}] - \sqrt{\pi} \frac{|h_1|}{|h_0|} \frac{\Gamma(l + \frac{1}{2})}{\Gamma(l)}}, \quad (48)$$

where Γ denotes the Gamma function. ■

Proof: See Appendix D. □

According to Theorem 4, the improvement factor of $\tilde{\mathbf{d}}_{\mathbf{y}_0}^{(n)}$ and $\tilde{\mathbf{d}}_{\mathbf{y}_1}^{(n)}$ depends on the length of the corresponding vectors l and the ratio of the channel gains h_0 and h_1 . Now, considering (45) together with Theorem 3 and Theorem 4, the improvement factor of the OFDM interference vectors $\mathbf{d}_{\mathbf{y}_0}^{(n)}$ and $\mathbf{d}_{\mathbf{y}_1}^{(n)}$ will be

$$\frac{\mathbb{E}\{\|\mathbf{d}_{\mathbf{y}_0}^{(n)} + \mathbf{d}_{\mathbf{y}_1}^{(n)}\|^2\}}{\mathbb{E}\{\min_{\theta} \|\mathbf{d}_{\mathbf{y}_0}^{(n)} + e^{j\theta} \mathbf{d}_{\mathbf{y}_1}^{(n)}\|^2\}} \approx \frac{2(1 + \frac{|h_1|^2}{|h_0|^2})}{2(1 + \frac{|h_1|^2}{|h_0|^2}) - \sqrt{\pi} \frac{|h_1|}{|h_0|} \frac{\Gamma(2.5)}{\Gamma(2)}}$$

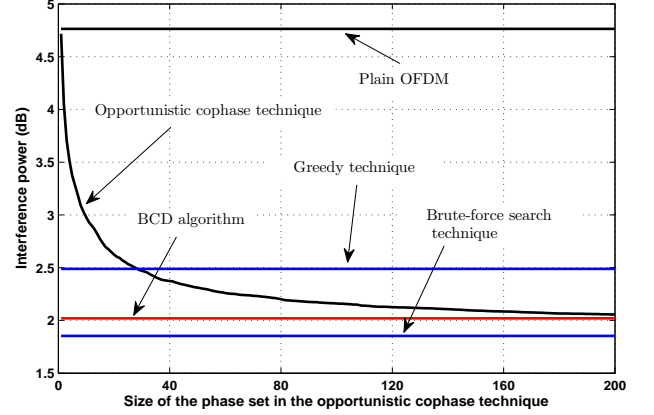


Fig. 5. Comparison of the proposed techniques for finding the optimal adjustment phases in the single-antenna case where $m = 3$.

$$\cong \frac{1 + \frac{|h_1|^2}{|h_0|^2}}{1 + \frac{|h_1|^2}{|h_0|^2} - 1.1781 \frac{|h_1|}{|h_0|}} \quad (49)$$

which depends on the ratio of channel fading gains h_1 and h_2 .

IV. SIMULATION RESULTS

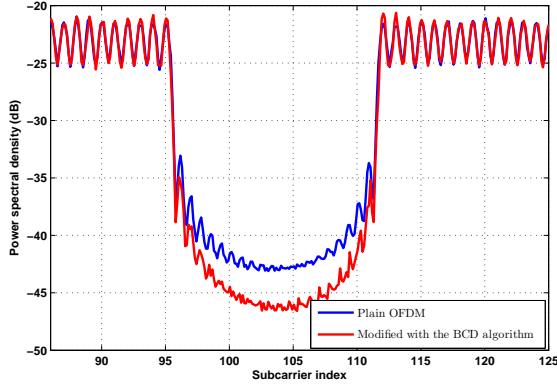
In this section, the performance of the proposed phase rotation technique for single-antenna and multi-antenna OFDM cognitive transmitters is investigated using numerical simulations. In simulations, for both single-antenna and multi-antenna cases, the cognitive systems employ OFDM signaling with $N = 256$ subcarriers and the spectrum is upsampled by a factor of $L = 8$. A number of subcarriers corresponding to the primary user bandwidth are deactivated and the remaining are BPSK-modulated.

A. Single-antenna OFDM Cognitive Transmitter

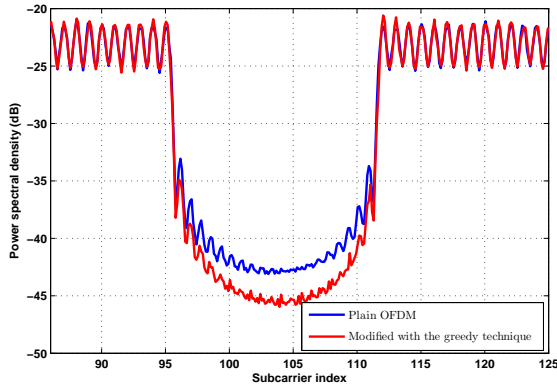
Fig. 5 shows the performance of the three proposed techniques in Section II-B for $m = 3$. Here the primary user bandwidth is assumed to be spread over $B = 16$ consecutive subcarriers from subcarrier 97 to 112. Also, for the BCD method we have run the simulations for 4 iterations. As can be observed from the figure, the block coordinate descent method has the best performance and reduces the interference by almost 3 dB on average. Moreover, the gap between the performance obtained using the BCD algorithm and the optimal performance of brute-force algorithm is negligible.

In order to show the performance of the proposed methods in reducing the spectrum at the primary band, the spectrum of the transmitted OFDM symbols is depicted in Fig. 6 where the spectrum of the plain OFDM signal is compared to the phase adjusted OFDM for $m = 3$.

The upper bound derived in Section II-C for the case of $m = 1$ is also evaluated numerically under two different primary activity configurations. In the first configuration, the primary user band is spread over 16 subcarriers that are located from subcarrier 121 to 136. We call this configuration 2-sided OFDM. In the second configuration, the primary user's band



(a)



(b)

Fig. 6. Power spectrum of the phase adjusted OFDM signal transmitted from a single-antenna cognitive transmitter where $m = 3$; (a): optimal phases are found using the BCD algorithm, (b): optimal phases are found using the greedy technique.

TABLE II
THE IMPROVEMENT FACTOR AND UPPER BOUND FOR 1-SIDED AND 2-SIDED OFDM SIGNALS

| | 1-sided OFDM | 2-sided OFDM |
|------------------|--------------|--------------|
| ξ (dB) | 2.1 | 1.9 |
| Upper bound (dB) | 2.7 | 2.4 |

is located at one end of the total OFDM signal bandwidth on the last 8 subcarriers. We call this configuration 1-sided OFDM. It can also be considered as out-of-band (OOB) radiation mitigation for current OFDM systems. Table II shows the improvement factors of the proposed technique for these OFDM configurations obtained from numerical simulations and the corresponding theoretical upper bounds. As can be seen from Table II, the upper bounds are relatively tight.

B. Multi-antenna OFDM Cognitive Transmitter

In the multi-antenna case, we first use numerical simulations to evaluate the analysis derived in Section III-C for the case of $M = 1$, i.e. two secondary transmitter antennas. Here the channels are Rayleigh fading, i.e., $|h_i|$ and $\angle h_i$ have Rayleigh and uniform distributions, respectively. In Fig. 7, the solid line shows the behavior of (49) vs. $\frac{|h_1|}{|h_0|}$. Computer

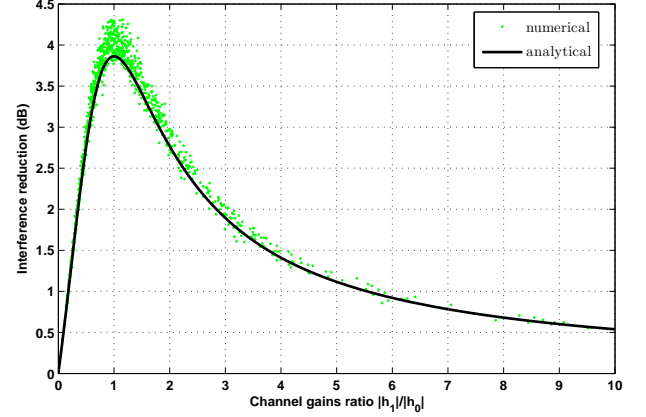


Fig. 7. Improvement of the proposed technique in interference reduction for different channel gains ratios $\frac{|h_1|}{|h_0|}$ for the multi-antenna case with two transmitter antennas.

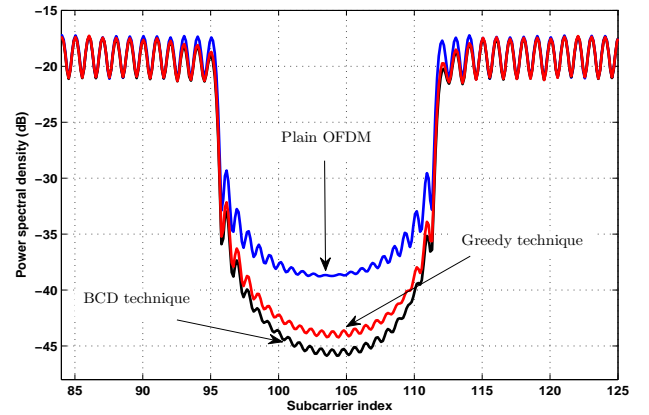


Fig. 8. Power spectrum of the phase adjusted OFDM signal transmitted from a 4-antenna cognitive transmitter using the BCD and the greedy technique.

simulations are used to find the interference reduction obtained by the proposed technique for different realizations of the channel gains h_0 and h_1 . The numerical results are shown in Fig. 7 as dots. In the simulations, the primary bandwidth is assumed to be spread over $B = 32$ consecutive subcarriers. As it can be seen in Fig. 7, numerical results approximately agree with the analytical results for the improvement of the proposed phase adjustment technique. The slight difference between the analytical and numerical results is attributed to the Gaussian assumption of the interference vectors, which is an approximation.

Fig. 8 illustrates the power spectral density of the received OFDM signals transmitted from 4 secondary antennas, i.e. $M = 3$, at the primary receiver. Here the primary user band is spread over 16 subcarriers from subcarrier 97 to 112. The performance of the BCD algorithm with 4 iterations and the greedy technique is shown in the figure. It can be seen from Fig. 8 that the proposed BCD algorithm for finding the optimal rotation phases decreases the interference to the primary user by up to 6 dB.

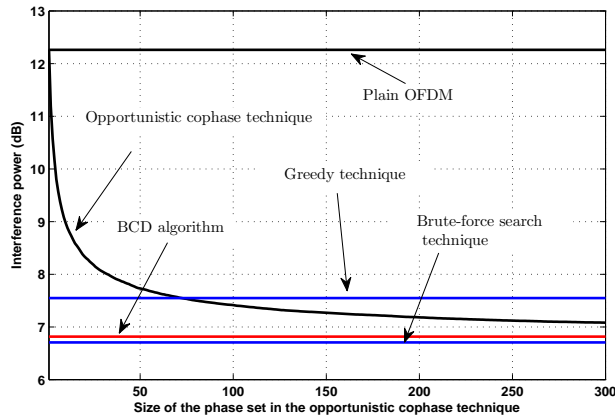


Fig. 9. Comparison of the proposed techniques for finding the optimal adjustment phases in the multiple-antenna case with four transmit antennas.

TABLE III

IMPROVEMENT OF THE PROPOSED TECHNIQUE FOR DIFFERENT CHANNEL MODELS.

| channel model | RMS delay spread (μs) | improvement (dB) |
|---------------|------------------------------------|------------------|
| flat fading | 0 | 3.23 |
| SUI-1 | 0.111 | 3.12 |
| SUI-3 | 0.264 | 2.84 |
| SUI-4 | 1.257 | 2.62 |

Finally, Fig. 9 gives a comparison of the performance of the proposed techniques for calculating the optimal rotation phases in Section III-B for the case of $M = 3$, i.e., 4 transmitter antennas. Here again 4 iterations are used in the BCD algorithm. Similar to the single-antenna case, the BCD algorithm outperforms the other techniques and yields close to optimal performance.

Frequency selective fading channels– The performance of the proposed phase rotation technique is also investigated under frequency selective channels using numerical simulations for a cognitive system with 3 transmit antennas. In frequency selective fading channels, each subcarrier in the OFDM symbols undergoes different fading. In other words, H_i , $i = 0, 1, 2$, are diagonal matrices whose diagonal entries are not necessarily equal. In computer simulations, H_i , $i = 0, 1, 2$, are modeled by the SUI-4 channel model [19] which is a tapped-delay-line model with 3 taps, and is suitable for MIMO broadband wireless applications. Moreover, the transmitter antennas are assumed to be sufficiently spatially separated. Therefore, the channels are generated independently. Here the primary user occupies a bandwidth of 16 subcarriers. The power spectral density of the received OFDM signal at the primary receiver is depicted in Fig. 10, which shows an improvement of approximately 6 dB in sidelobe reduction using the BCD algorithm for finding the adjustment phases.

Furthermore, the performance of the proposed phase adjustment technique for a 2-antenna secondary transmitter using different frequency selective channel models with different delay spreads is investigated. For each channel model, the median improvement over 2000 realizations of the channels

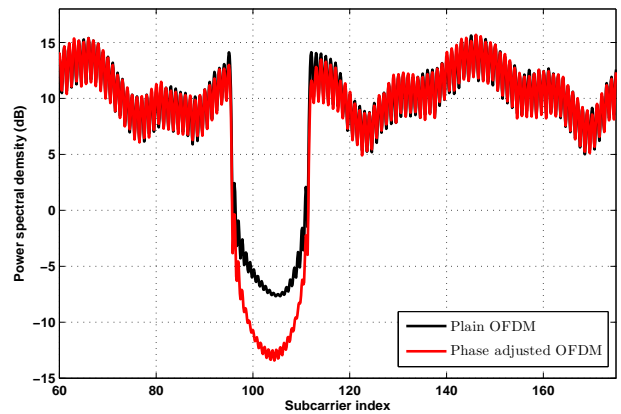


Fig. 10. Spectrum of the received OFDM signals transmitted from three antennas with frequency selective fading channels. Adjustment phases are calculated using the BCD algorithm.

is computed. The results are shown in Table III. It is observed from Table III that for channels with different delay spreads, the improvements are in approximate agreement with 3.23 dB for flat fading channels. However, as the delay spread is reduced, the performance improvement is better predicted by that of the flat fading results.

V. CONCLUSION

A new technique to reduce the interference to the primary users in single-antenna and multi-antenna transmitter OFDM cognitive radios has been presented. In the single-antenna case, the proposed phase-adjustment technique rotates all subcarriers of m consecutive OFDM symbols based on the prior OFDM symbols, such that the entire interference is minimized. In the multi-antenna case, transmitted symbols of one antenna are rotated in the complex space such that the interference to the primary receiver is minimized. The technique does not suffer from existing drawbacks such as loss in useful data rate, increase in BER, and high complexity. Moreover, the performance of the technique is evaluated analytically for both single-antenna and multi-antenna OFDM cognitive systems and verified by computer simulations.

APPENDIX A

PROOF OF THEOREM 1

We can expand the right hand side of (8) as

$$\begin{aligned}
 & \arg \min_{\theta} \|\mathbf{d}^{(n)} + e^{j\theta} \mathbf{d}^{(n+1)}\|^2 \\
 &= \arg \min_{\theta} \{ \|\mathbf{d}^{(n)}\|^2 + \|\mathbf{d}^{(n+1)}\|^2 + \langle \mathbf{d}^{(n)}, \mathbf{d}^{(n+1)} \rangle e^{j\theta} \\
 & \quad + \langle \mathbf{d}^{(n)}, \mathbf{d}^{(n+1)} \rangle e^{-j\theta} \} \\
 &= \arg \min_{\theta} (2\Re\{ \langle \mathbf{d}^{(n)}, \mathbf{d}^{(n+1)} \rangle e^{j\theta} \}). \tag{50}
 \end{aligned}$$

The argument in (50) is minimized when $\arg(\langle \mathbf{d}^{(n)}, \mathbf{d}^{(n+1)} \rangle e^{j\theta}) = \pi$. Hence,

$$\theta = \pi - \arg(\langle \mathbf{d}^{(n)}, \mathbf{d}^{(n+1)} \rangle) \tag{51}$$

APPENDIX B
PROOF OF THEOREM 2

The numerator of the right hand side of (18) is expanded as

$$\begin{aligned} \mathbb{E}\{\|\mathbf{d}^{(n)} + \mathbf{d}^{(n+1)}\|^2\} &= \mathbb{E}\{\|\mathbf{d}^{(n)}\|^2\} + \mathbb{E}\{\|\mathbf{d}^{(n+1)}\|^2\} \quad (52) \\ &= 2 \sum_{i=1}^K \lambda_i, \quad (53) \end{aligned}$$

where (52) follows from the fact that $\mathbf{d}^{(n)}$ and $\mathbf{d}^{(n+1)}$ are zero-mean and independent. Similarly, we can expand the denominator of the right hand side of (18) as

$$\begin{aligned} &\mathbb{E}\{\min_{\theta} \|\mathbf{d}^{(n)} + e^{j\theta} \mathbf{d}^{(n+1)}\|^2\} \\ &= \mathbb{E}\{\|\mathbf{d}^{(n)}\|^2 + \|\mathbf{d}^{(n+1)}\|^2 + \min_{\theta} [2\Re(e^{j\theta} \mathbf{d}^{(n)\dagger} \mathbf{d}^{(n+1)})]\} \\ &= \mathbb{E}\{\|\mathbf{d}^{(n)}\|^2\} + \mathbb{E}\{\|\mathbf{d}^{(n+1)}\|^2\} - 2\mathbb{E}|\mathbf{d}^{(n)\dagger} \mathbf{d}^{(n+1)}|, \quad (54) \end{aligned}$$

where (54) follows by choosing a proper θ to minimize $\Re(e^{j\theta} \mathbf{d}^{(n)\dagger} \mathbf{d}^{(n+1)})$. Now, $\mathbb{E}|\mathbf{d}^{(n)\dagger} \mathbf{d}^{(n+1)}|$ can be upper-bounded as

$$\begin{aligned} \mathbb{E}|\mathbf{d}^{(n)\dagger} \mathbf{d}^{(n+1)}|^2 &\leq \mathbb{E}|\mathbf{d}^{(n)\dagger} \mathbf{d}^{(n+1)}|^2 \\ &= \mathbb{E}|\mathbf{a}^\dagger U^\dagger \tilde{D}_1 U \mathbf{b}|^2 \\ &= \mathbb{E}\{\text{Tr}(\mathbf{a}^\dagger U^\dagger \tilde{D}_1 U \mathbf{b} \mathbf{b}^\dagger U^\dagger \tilde{D}_1^\dagger U \mathbf{a})\} \\ &= \mathbb{E}\{\text{Tr}(U \mathbf{a} \mathbf{a}^\dagger U^\dagger \tilde{D}_1 U \mathbf{b} \mathbf{b}^\dagger U^\dagger \tilde{D}_1^\dagger)\} \\ &= \text{Tr}(U \Sigma U^\dagger \tilde{D}_1 U \Sigma U^\dagger \tilde{D}_1^\dagger) \\ &= \text{Tr}(R_n R_{n+1}). \quad (55) \end{aligned}$$

Therefore, by applying (55) to (54), the upper bound is proved.

APPENDIX C
PROOF OF THEOREM 3

The covariance matrices $R_{\mathbf{y}_1}$ and $R_{\mathbf{y}_2}$ are diagonalized as

$$Q^\dagger R_{\mathbf{y}_0} Q = \text{diag}(\{\lambda_i\}_{i=1}^K), \quad (56)$$

$$Q^\dagger R_{\mathbf{y}_1} Q = \text{diag}(\{\frac{|h_1|^2}{|h_0|^2} \lambda_i\}_{i=1}^K), \quad (57)$$

where $Q = [\mathbf{q}_1 \ \mathbf{q}_2 \ \dots \ \mathbf{q}_K]$ is the eigenvector matrix of $R_{\mathbf{y}_1}$ and $R_{\mathbf{y}_2}$, and is unitary. Thus, $\mathbf{d}_{\mathbf{y}_0}^{(n)}$ and $\mathbf{d}_{\mathbf{y}_1}^{(n)}$ can be expressed as

$$\mathbf{d}_{\mathbf{y}_j}^{(n)} = \sum_{i=1}^K \tilde{d}_{ji} \mathbf{q}_i, \quad j = 0, 1, \quad (58)$$

where \tilde{d}_{0i} and \tilde{d}_{1i} are independent Gaussian random variables with $\tilde{d}_{0i} \sim \mathcal{CN}(0, \lambda_i)$, $\tilde{d}_{1i} \sim \mathcal{CN}(0, \frac{|h_1|^2}{|h_0|^2} \lambda_i)$, $i = 1, \dots, K$. Thus, the numerator on the left hand side of (42) can be written as

$$\begin{aligned} \mathbb{E}\{\|\mathbf{d}_{\mathbf{y}_0}^{(n)} + \mathbf{d}_{\mathbf{y}_1}^{(n)}\|^2\} &= \mathbb{E}\{\|\sum_{i=1}^K \tilde{d}_{0i} \mathbf{q}_i + \sum_{i=1}^K \tilde{d}_{1i} \mathbf{q}_i\|^2\} \\ &= \sum_{i=1}^K \lambda_i + \sum_{i=1}^K \frac{|h_1|^2}{|h_0|^2} \lambda_i \\ &\approx \mathbb{E}\{\sum_{i=1}^l (|\tilde{d}_{0i}|^2 + |\tilde{d}_{1i}|^2)\} \end{aligned}$$

$$= \mathbb{E}\{\|\tilde{\mathbf{d}}_{\mathbf{y}_0}^{(n)} + \tilde{\mathbf{d}}_{\mathbf{y}_1}^{(n)}\|^2\}. \quad (59)$$

Similarly, the denominator on the left hand side of (42) is expanded as

$$\begin{aligned} &\mathbb{E}\{\min_{\theta} \|\mathbf{d}_{\mathbf{y}_0}^{(n)} + e^{j\theta} \mathbf{d}_{\mathbf{y}_1}^{(n)}\|^2\} \\ &= \mathbb{E}\{\min_{\theta} \|\sum_{i=1}^K \tilde{d}_{0i} \mathbf{q}_i + e^{j\theta} \sum_{i=1}^K \tilde{d}_{1i} \mathbf{q}_i\|^2\} \\ &= \mathbb{E}\{\sum_{i=1}^K (|\tilde{d}_{0i}|^2 + |\tilde{d}_{1i}|^2) + \min_{\theta} \sum_{i=1}^K (e^{j\theta} \tilde{d}_{0i}^* \tilde{d}_{1i} + e^{-j\theta} \tilde{d}_{0i} \tilde{d}_{1i}^*)\} \\ &= \mathbb{E}\{\sum_{i=1}^K (|\tilde{d}_{0i}|^2 + |\tilde{d}_{1i}|^2) + 2 \min_{\theta} [\Re(\sum_{i=1}^K e^{j\theta} \tilde{d}_{0i}^* \tilde{d}_{1i})]\} \\ &\approx \mathbb{E}\{\sum_{i=1}^l (|\tilde{d}_{0i}|^2 + |\tilde{d}_{1i}|^2) - 2|\sum_{i=1}^l \tilde{d}_{0i}^* \tilde{d}_{1i}|\} \\ &= \mathbb{E}\{\min_{\theta} \|\tilde{\mathbf{d}}_{\mathbf{y}_0}^{(n)} + e^{j\theta} \tilde{\mathbf{d}}_{\mathbf{y}_1}^{(n)}\|^2\}, \quad (60) \end{aligned}$$

and the proof is complete.

APPENDIX D
PROOF OF THEOREM 4

The numerator of the left hand side of (48) is expanded as

$$\mathbb{E}\{\|\tilde{\mathbf{d}}_{\mathbf{y}_0}^{(n)} + \tilde{\mathbf{d}}_{\mathbf{y}_1}^{(n)}\|^2\} = \mathbb{E}\{\|\tilde{\mathbf{d}}_{\mathbf{y}_0}^{(n)}\|^2\} + \mathbb{E}\{\|\tilde{\mathbf{d}}_{\mathbf{y}_1}^{(n)}\|^2\} \quad (61)$$

$$= l\lambda_1 + l \frac{|h_1|^2}{|h_0|^2} \lambda_1, \quad (62)$$

where (61) follows from the fact that $\tilde{\mathbf{d}}_{\mathbf{y}_1}^{(n)}$ and $\tilde{\mathbf{d}}_{\mathbf{y}_2}^{(n)}$ are zero-mean and independent.

Similarly, we expand the denominator as

$$\begin{aligned} &\mathbb{E}\{\min_{\theta} \|\tilde{\mathbf{d}}_{\mathbf{y}_0}^{(n)} + e^{j\theta} \tilde{\mathbf{d}}_{\mathbf{y}_1}^{(n)}\|^2\} \\ &= \mathbb{E}\{\min_{\theta} [\|\tilde{\mathbf{d}}_{\mathbf{y}_0}^{(n)}\|^2 + \|\tilde{\mathbf{d}}_{\mathbf{y}_1}^{(n)}\|^2 + e^{j\theta} \tilde{\mathbf{d}}_{\mathbf{y}_0}^{(n)\dagger} \tilde{\mathbf{d}}_{\mathbf{y}_1}^{(n)} + e^{-j\theta} \tilde{\mathbf{d}}_{\mathbf{y}_1}^{(n)\dagger} \tilde{\mathbf{d}}_{\mathbf{y}_0}^{(n)}]\} \\ &= \mathbb{E}\{\|\tilde{\mathbf{d}}_{\mathbf{y}_0}^{(n)}\|^2 + \|\tilde{\mathbf{d}}_{\mathbf{y}_1}^{(n)}\|^2 + \min_{\theta} [2\Re\{e^{j\theta} \tilde{\mathbf{d}}_{\mathbf{y}_0}^{(n)\dagger} \tilde{\mathbf{d}}_{\mathbf{y}_1}^{(n)}\}]\} \quad (63) \end{aligned}$$

$$= \mathbb{E}\{\|\tilde{\mathbf{d}}_{\mathbf{y}_0}^{(n)}\|^2\} + \mathbb{E}\{\|\tilde{\mathbf{d}}_{\mathbf{y}_1}^{(n)}\|^2\} - 2\mathbb{E}\{\|\tilde{\mathbf{d}}_{\mathbf{y}_0}^{(n)\dagger} \tilde{\mathbf{d}}_{\mathbf{y}_1}^{(n)}\|\}, \quad (64)$$

where (64) follows by choosing θ to minimize the argument inside (63).

Due to rotational symmetry of $\tilde{\mathbf{d}}_{\mathbf{y}_0}^{(n)}$ and $\tilde{\mathbf{d}}_{\mathbf{y}_1}^{(n)}$, without loss of generality, we may assume that the vector $\tilde{\mathbf{d}}_{\mathbf{y}_0}^{(n)}$ is along the first coordinate \mathbf{e}_1 of the l -dimensional complex space, i.e., $\tilde{\mathbf{d}}_{\mathbf{y}_0}^{(n)} = \|\tilde{\mathbf{d}}_{\mathbf{y}_0}^{(n)}\| \mathbf{e}_1$. Therefore, (64) can be written as

$$\begin{aligned} &\mathbb{E}\{\|\tilde{\mathbf{d}}_{\mathbf{y}_0}^{(n)}\|^2\} + \mathbb{E}\{\|\tilde{\mathbf{d}}_{\mathbf{y}_1}^{(n)}\|^2\} - 2\mathbb{E}\{\|\tilde{\mathbf{d}}_{\mathbf{y}_0}^{(n)}\| \|\mathbf{e}_1^\dagger \tilde{\mathbf{d}}_{\mathbf{y}_1}^{(n)}\|\} \\ &= l\lambda_1 + l \frac{|h_1|^2}{|h_0|^2} \lambda_1 - 2\mathbb{E}\{\|\tilde{\mathbf{d}}_{\mathbf{y}_0}^{(n)}\|\} \mathbb{E}\{\|\tilde{d}_{11}\|\} \quad (65) \end{aligned}$$

$$= l\lambda_1 + l \frac{|h_1|^2}{|h_0|^2} \lambda_1 - \left(\sqrt{2\lambda_1} \frac{\Gamma(\frac{2l+1}{2})}{\Gamma(l)} \right) \frac{|h_1|}{|h_0|} \sqrt{\lambda_1} \sqrt{\frac{\pi}{2}} \quad (66)$$

$$= l\lambda_1 + l \frac{|h_1|^2}{|h_0|^2} \lambda_1 - \sqrt{\pi} \sqrt{\lambda_1} \frac{|h_1|}{|h_0|} \sqrt{\lambda_1} \frac{\Gamma(l + \frac{1}{2})}{\Gamma(l)} \quad (67)$$

where \tilde{d}_{11} is the first coordinate of $\tilde{\mathbf{d}}_{y_1}^{(n)}$ and (65) follows from independence of $\tilde{\mathbf{d}}_{y_0}^{(n)}$ and $\tilde{\mathbf{d}}_{y_1}^{(n)}$. Also, since $\tilde{\mathbf{d}}_{y_0}^{(n)}$ and $\tilde{\mathbf{d}}_{y_1}^{(n)}$ are i.i.d. complex Gaussian vectors, $\|\tilde{\mathbf{d}}_{y_0}^{(n)}\|/\sqrt{\lambda_1}$ is a chi-distributed and $|\tilde{d}_{11}|$ is a Rayleigh random variable. Hence, (66) follows, and the proof is complete.

REFERENCES

- [1] E. H. M. Alian and P. Mitran, "Interference Mitigation in MIMO-OFDM Cognitive Radio Systems Using Phase Rotation," in *IEEE Wireless Communications and Networking Conference, WCNC*, April 2012.
- [2] T. Weiss and F. Jondral, "Spectrum pooling: an innovative strategy for the enhancement of spectrum efficiency," *Communications Magazine, IEEE*, vol. 42, pp. S8 – 14, Mar. 2004.
- [3] T. Weiss, J. Hillenbrand, A. Krohn, and F. Jondral, "Mutual interference in OFDM-based spectrum pooling systems," in *Vehicular Technology Conference, 2004. VTC 2004-Spring. 2004 IEEE 59th*, vol. 4, pp. 1873 – 1877, May 2004.
- [4] P. Tan and N. Beaulieu, "Reduced ICI in OFDM systems using the "better than" raised-cosine pulse," *Communications Letters, IEEE*, vol. 8, pp. 135 – 137, Mar. 2004.
- [5] A. Assalini and A. Tonello, "Improved Nyquist pulses," *Communications Letters, IEEE*, vol. 8, pp. 87 – 89, Feb. 2004.
- [6] I. Cosovic, S. Brandes, and M. Schnell, "Subcarrier weighting: a method for sidelobe suppression in OFDM systems," *Communications Letters, IEEE*, vol. 10, pp. 444 – 446, June 2006.
- [7] I. Cosovic and T. Mazzoni, "Suppression of sidelobes in OFDM systems by multiple-choice sequences," *European Transactions on Telecommunications*, vol. 17, pp. 623–630, June 2006.
- [8] H. Yamaguchi, "Antenna interference cancellation technique for MB-OFDM cognitive radio," in *Microwave Conference, 2004. 34th European*, vol. 2, pp. 1105 – 1108, Oct. 2004.
- [9] H. Mahmoud and H. Arslan, "Sidelobe suppression in OFDM-based spectrum sharing systems using adaptive symbol transition," *Communications Letters, IEEE*, vol. 12, pp. 133 – 135, Feb. 2008.
- [10] J. van de Beek and F. Berggren, "N-continuous OFDM," *Communications Letters, IEEE*, vol. 13, pp. 1 – 3, January 2009.
- [11] Y. Wang and J. Coon, "Active interference cancellation for systems with antenna selection," in *Communications, 2008. ICC '08. IEEE International Conference on*, pp. 3785 – 3789, May 2008.
- [12] F. Sarabchi and C. Nerguizian, "Interference cancellation technique for MIMO MB-OFDM UWB cognitive radio," in *Wireless and Mobile Communications (ICWMC), 2010 6th International Conference on*, pp. 472 – 477, 2010.
- [13] Q. Liang, Y. Xiao, X. He, and S. Li, "Iterative estimation and cancellation of N-continuous distortion for MIMO OFDM systems," in *Wireless Communications and Signal Processing (WCSP), 2010 International Conference on*, pp. 1 – 4, Oct. 2010.
- [14] D. Petrovic, W. Rave, and G. Fettweis, "Common phase error due to phase noise in OFDM-estimation and suppression," in *Personal, Indoor and Mobile Radio Communications, 2004. PIMRC 2004. 15th IEEE International Symposium on*, vol. 3, pp. 1901 – 1905 Vol.3, 2004.
- [15] G. Sridharan and T. J. Lim, "Blind estimation of common phase error in OFDM and OFDMA," in *GLOBECOM 2010, 2010 IEEE Global Telecommunications Conference*, pp. 1 – 5, 2010.
- [16] M. H. Hayes, *Statistical Digital Signal Processing and Modeling*. Wiley, 1996.
- [17] D. Bertsekas, *Nonlinear programming*. Athena Scientific, 1999.
- [18] M. Xia, W. Wen, and S. Kim, "Opportunistic cophasing transmission in MISO systems," *Communications, IEEE Transactions on*, vol. 57, no. 12, pp. 3764–3770, 2009.
- [19] *Channel Models for Fixed Wireless Applications (IEEE802.16.3c-01/29r4)*. IEEE P802.16, 2001.



Ehsan Haj Mirza Alian (S'11) received his BSc. and MSc. in Electrical Engineering (Communication systems), in 2005 and 2008, respectively, from Isfahan University of Technology, Isfahan, Iran. He is currently working towards his Ph.D. degree at the Department of Electrical and Computer Engineering, University of Waterloo, Canada. His research interests include wireless communications, information theory, signal processing, and cognitive radio networks.



Patrick Mitran (S'01, M'07, SM'13) received the Bachelor's and Master's degrees in electrical engineering, in 2001 and 2002, respectively, from McGill University, Montreal, PQ, Canada, and the Ph.D. degree from the Division of Engineering and Applied Sciences, Harvard University, Cambridge, MA in 2006. In 2005, he interned as a research scientist for Intel Corporation in the Radio Communications Lab. In 2006-07 he was an applied mathematics lecturer in the School of Engineering and Applied Sciences, Harvard University. He is currently an Associate

Professor in the Department of Electrical and Computer Engineering at the University of Waterloo, Waterloo, Ontario, Canada. His research interests are in the areas of information theory, wireless communications and coding.

Dr. Mitran is a licensed Professional Engineer in the Province of Ontario and was awarded the Government of Ontario Early Researcher Award in 2011. He currently serves as an Editor for the *IEEE TRANSACTIONS ON COMMUNICATIONS* in the area of Networking and Cross-Layer Design.